Journal of Fusion Energy
https://doi.org/10.1007/s10894-018-0194-x

ORIGINAL RESEARCH

# Evolution of the Pinched Column During Hard X-ray and Neutron Emission in a Dense Plasma Focus

P. Kubes[1] · M. Paduch[2] · M. J. Sadowski[2,3] · J. Cikhardt[1] · B. Cikhardtova[1] · D. Klir[1] · J. Kravarik[1] · V. Munzar[1] · K. Rezac[1] · E. Zielinska[2] · E. Skladnik-Sadowska[3] · A. Szymaszek[2] · K. Tomaszewski[4] · D. Zaloga[3]



**Abstract**
The paper summarizes important results of the recent experimental studies performed on the plasma-focus PF-1000 facility operated in Warsaw, Poland, mainly with the pure deuterium filling. Attention is focused on the evolution of toroidal and plasmoidal self-organized structures formed by internal closed currents inside the dense plasma column. The production of hard x-rays and neutrons corresponds with the formation and decay of plasmoids, in which charged particles can be accelerated effectively to high energies, during a release of the magnetic energy from current filaments of high energy density. It is noticed that the studies of laboratory fusion and cosmic plasmas deal with similar problems, e.g., the fast release of the magnetic energy in a form of high-energy charged particle beams.

**Keywords** Plasma focus · Neutron source · Magnetic reconnection · Self-generation

## Introduction

Research on fusion plasmas produced in tokamaks or during interactions of powerful lasers with solid targets, as well as studies of z-pinch discharges and astrophysical jets—tries to solve a similar problem, namely the generation of high energy electrons and ions by mechanisms which have not been explained so far completely. Plasmas generated by plasma focus (PF) discharges have some advantages which can facilitate the solving of this problem, because they have parameters convenient for complementary diagnostics with good temporal-, spatial-, and energetic-resolution. When the deuterium filling is applied, the primary deuterons can reach energies sufficient for efficient fusion DD reactions, which can generate fast neutrons. These fusion-produced neutrons, together with hard x-rays (HXR) produced by fast electrons, provide an indirect information about the charged particles accelerated in plasma.

The comprehensive diagnostics applied in PF experiments have made it possible: (1) to determine instants of the generation and energies of the accelerated charged particles, (2) to observe organized structures of plasma and their spatial- and temporal-evolution, and (3) to describe their correlations with the HXR and fusion-neutron production.

In discharges of the Z-pinch type, as well as in PF-type experiments, the current of MA intensity, which flows through the plasma along the z-axis, forms its own magnetic field, which compresses plasma, usually with a relatively good axial symmetry. The plasma column of dimensions ranging several centimetres is usually compressed during hundreds nanosecond, reaching an electron temperature above (100–200) eV, and electron density above $10^{24}$ $m^{-3}$. The compression of a current sheath is accompanied by the conversion of a part of the kinetic energy into magnetic one associated with closed currents. This magnetic field is later released in a form of fast

✉ P. Kubes
kubes@fel.cvut.cz

[1] Czech Technical University, 166-27 Prague, Czech Republic

[2] Institute of Plasma Physics and Laser Microfusion, 01-497 Warsaw, Poland

[3] National Centre for Nuclear Research, 05-400 Otwock-Świerk, Poland

[4] ACS Ltd, 01-497 Warsaw, Poland

Published online: 08 October 2018

electrons and ions which can reach observed energy of hundreds keV [1–4].

Therefore, the main aim of this paper was to analyze evolution of organized structures, formed by closed currents with poloidal and toroidal components, and corresponding magnetic fields in the time of the HXRs and neutrons production. It should shed some light on specific features of the plasma transformation processes and mechanisms of the charged particle acceleration.

Experimental findings, concerning the release of the magnetic energy in the organized plasma structures in PF-discharges, can be an inspiration for researchers of tokamaks and laser-fusion experiments, as well as for the astrophysical community.

## Experimental Set-Up and Diagnostics

The described studies have concerned plasma produced within the PF-1000 facility operated at the IPPLM in Warsaw, Poland [5–12]. The investigated discharges, as reported in this paper, were carried out at the deuterium filling. Plasmas had electron densities transparent for interferometric measurements in the visible wavelength region. The plasma transformation velocity, equal to $(1–2) \times 10^5$ m/s, made it possible to perform a detailed diagnostics with a temporal resolution of the order of 3 ns, and the spatial resolution of the order of 1 mm. A laser interferometric system enabled plasma internal structures to be observed, because it could record 15 frames from each shot, during the plasma evolution from the implosion phase to its decay [7].

Energy stored in a capacitor bank amounted to (250–350) kJ, and the peak current reached (1–2) MA. Time-resolved soft X-ray (SXR) signals were investigated with a filtered silicon PIN detector, which recorded photons of energy above 700 eV. Three scintillation detectors recorded the hard X-ray (HXR) and neutron signals lasting several tens ns, when measured side-on and in the both axial directions, at a distance of about 7 m from the pinch centre. Those detectors made it possible to determine instants of the emission of HXRs and fusion-produced neutrons, as well as to estimate their anisotropy and a mean neutron velocity, using a time-of-flight method [8]. The interferometric frames were recorded subsequently with a delay equal to 10 ns or 20 ns, during a period lasting 210 ns [9]. The applied laser interferometer used parallel mirrors in the Mach–Zehnder configuration without any wedge, and for shots without plasma it formed an image with widely distributed interferometric fringes. For shots with plasma, the closed dense fringes indicated regions of the density extremes. In some shots, absolute calibrated magnetic probes were placed in the anode front-plate at different radial distances from the z-axis, and recorded the azimuthal and axial components of the magnetic field [10, 11]. Electron temperature values were estimated from intensities of spectral lines which were emitted by H- and He-like ions of impurities C, N, and O, and recorded by means of an EUV spectrometer [12].

The presented results summarize results of 16 campaigns, which were performed during recent 8 years, when more than 1000 discharges were investigated. For the analysis of results we selected the shots of typical features and regularity.

## Characteristics of the Recorded Fusion Neutrons

Particular attention was focused first on the studies of HRXs and fusion-neutrons. Typical HXRs and neutron signals are shown in Fig. 1.

The recorded waveforms showed usually two HXR peaks and two neutron signals. The beginnings of the these neutron signals (N1 and N2) corresponded to the beginnings of the corresponding HXR signals. The scintillation detectors, which were placed at the distance of 7 m from the pinch centre, recorded the fusion-produced neutrons (of an average energy equal to 2.45 MeV) with a delay of 300 ns. The first (HXR1) and neutron pulses (N1) were emitted at the stopping of the current sheath implosion, while the next pulses (HXR2 and N2) were produced during and after an interruption of the dense pinch column, which could occur several times.

The neutron signal, which was recorded in the downstream direction (i.e. along the z-axis), had the maximum delayed by less than 300 ns. It was caused by motion of fast deuterons (responsible for the neutrons production) in

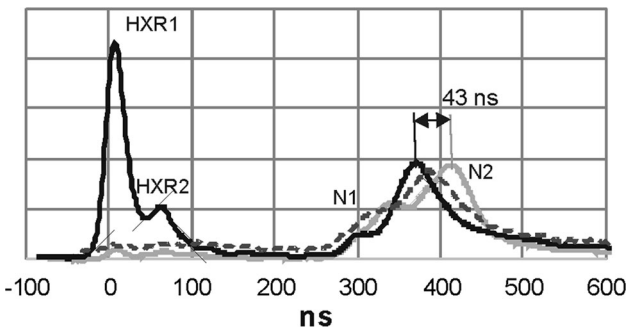


**Fig. 1** Shot #8600. Two pulses of HXRs (HXR1, HXR2) and two neutron signals (N1, N2) recorded with the scintillation detectors placed at a distance of 7 m in front of the electrodes outlets in the downstream direction (black), behind the electrodes collector, i.e. in the upstream direction (shadow), and side-on (dashed). The shift marked by arrows shows the difference between the subsequent neutron peaks of the axial signals

the downstream direction mainly. The differences between the both neutron peaks, as measured in the downstream and upstream directions, were about (40–50) ns and corresponded to the mean deuteron velocity of (3–4.5) $\times$ $10^6$ m/s and deuteron energy equal to about (100–200) keV.

Taking into consideration the observed velocity of deuterons and their anisotropy, one could deduce that the neutrons were produced by the beam-target mechanism. The HXRs pulses were produced by fast electrons, which bombarded the anode-surface and had a similar energy distribution as the deuterons, but were emitted mainly in the upstream direction. The start of the HXR pulse after the electrons acceleration was estimated to be about 2 ns (for 50 cm flight to the anode). The number of fast deuterons needed for the total neutron yield of the order of $10^{10}$–$10^{11}$ per shot was calculated on the basis of the known cross-section of DD reaction, the mean energy of deuterons (equal to about 200 keV), the mean ion density (about $3 \times 10^{24}$ $m^{-3}$) and the assumed dimensions of the target. It amounted to about 1% of all deuterons contained inside the pinch column. Their energy was evaluated to be a few percentages of energy stored in the condenser bank [13].

Scattered neutrons, which were estimated to amount to about 20% of the total neutron yield [8], affected the tail of the neutron signals mainly. The total neutron yield changed from shot to shot within the range of one order of magnitude. This variation was caused by stochastic differences in the evolution of an individual shot from the breakdown to the pinch phase, probably due to some azimuthal asymmetry of the current sheath. The neutron signals and the total neutron yield could also be affected by the electrode configuration. For example, the neutron yield was considerably increased in shots performed after the fixing of an additional conical tip upon the anode end-plate. On the other hand, the neutron yield was decreased when an anti-anode was applied, despite of a higher energy density in the pinched column. The described changes in the electrode configuration, which were realized during (50–70) shots, did not change the main features of the neutron emission considerably.

It should be added that the fusion neutrons could also be produced in a rare and cold deuterium gas inside the discharge chamber. Their contribution was evaluated to amount to about 10% of the total neutron yield. The emission of such neutrons (at a distance of the order of 2 m from the plasma-focus centre) could be delayed by hundreds ns, and it (together with the scattered neutrons) could be responsible for long tails of time-resolved neutron signals.

## Organized Structures in the Dense Plasma Column

The applied laser interferometry system made it possible to estimate distributions of the electron density in the observed quasi-symmetrical toroidal and plasmoidal plasma structures, and to correlate their evolution with instants of the HXR and neutron emission. As an example one can concern two interferometric images obtained from shot #11452, which are shown in Fig. 2.

The presented interferometric frames show typical toroidal (Fig. 2a) and plasmoidal (Fig. 2b) structures. The radial distribution of the electron density inside the toroidal structure, as calculated by means of the Abel transformation of the recorded interferometric fringes in the chosen cross-section, reached the maximal values of about $1.2 \times 10^{24}$ $m^{-3}$ at the axis of the toroidal structure, and $3.5 \times 10^{24}$ $m^{-3}$ at the centre of the plasmoidal structure, respectively.

The electron temperature was estimated from a ratio of H- and He-like Lyman α-lines of C-, N- and O-ions. It reached (50–150) eV [12]. The value above 100 eV was also obtained at the instance of the peak of SXRs recorded by means of a PIN detector. The known plasma density and electron temperature values made it possible to estimate that a relaxation time of the electron and ion temperatures [4] was about 20 ns. Hence, one can assume that (at slower transformations) the conditions inside the considered plasma structures were quasi-stationary during several tens nanoseconds.

The known radial distribution of the electron density $n_e$, which was determined in two cross-sections (marked by white dashed lines in Fig. 2a, b), and the evaluated electron temperatures $T_e$ (on average about 70 eV) made it possible to estimate the plasma pressure in the toroidal and poloidal structures, as shown by grey and black curves in Fig. 2c, respectively.

The smooth shapes of the interferometric fringes and pressure gradient mentioned above could also indicate that the organized structure were created by closed internal currents. The formation of such organized structures was possible due to a magnetic dynamo effect in discharges with high Reynolds magnetic numbers, characterizing a strong magnetic field frozen in plasma, and ranging to $10^3$. It showed the dominant role of an advection term in a comparison with a diffusion term for the magnetic field. For the whole pinch column the diffusion time was calculated to be of the order of 100 μs, i.e. much longer than the duration of the PF discharge. That value decreased, however, rapidly with the plasma dimensions and it reached about 10 ns at the dimension about 100 μm, i.e. much larger than the Debye length (equal to about $10^{-8}$ m).

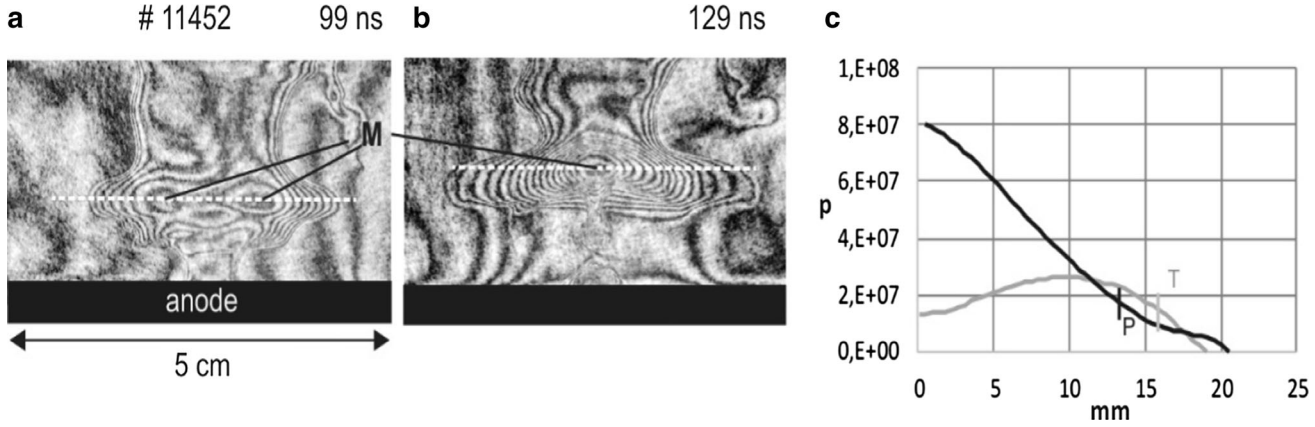


**Fig. 2** Shot #11452; **a** Interferometric images of the toroidal structure recorded at 99 ns, **b** the plasmoidal structure recorded 30 ns later, and **c** a radial distribution of the plasma pressure p (in Pa units), as calculated for temperature of 70 eV along the cross-sections lines marked in the images **a**, **b**. The letter M and black lines indicate positions of the density maxima, and the letters P and T show the boundary radii of the plasmoidal and toroidal structures, respectively

The dimension of 100 μm corresponded as to the Larmor radius, as well as to a mean free path for electron–ion collisions, and to a deuteron skin layer. Consequently, it determined the spatial scale of microturbulences and collision-free plasma. It should be noted that the anisotropy of internal structures could also be influenced by high magnetization of electrons (ranging 20). In contrary, the magnetization of deuterons reached the value equal to about 1 only [4].

A high gradient of the plasma pressure in the considered organized structures was probably produced by the closed currents and their magnetic fields [7]. The dominant current inside the toroidal plasma structure could flow in the toroidal direction, having a small poloidal stabilizing component, similar as in the toroidal pinch or tokamak discharge. The current inside the plasmoidal structure should have the poloidal form, stabilized by a smaller toroidal component. At considering quasi-stationary conditions, the plasma pressure in the ordered structures was evidently compensated by the pinching pressure of the current flowing through the plasma column surface in an agreement with the virial theorem [14]. Hence, the pressure values (determined in points T and P shown in Fig. 2c) made it possible to estimate that the magnetic field $B$ ranged up to 10 T, and the internal current $I$ was of the order of hundred kA [15]. For those estimations the use was made of the known equations:

$$2n_e kT_e \approx B^2/2\mu \quad \text{and} \quad B \approx \mu I/2\pi r \tag{1}$$

where $r$ means the radius and $\mu$ permeability. That value of the magnetic field was consistent with results of the experimental measurements performed by means of the absolute calibrated magnetic probes located within the anode end-plate [10, 11, 16]. Those measurements (carried out during 25 shots) showed the presence of a weak axial component of the magnetic field, which was generated spontaneously in front and in the imploding current sheath, as well as in the internal plasma structures.

## Transformations of Organized Structures and Acceleration of Charged Particles

The interferometric images (shown in Fig. 2a, b) presented two basic plasma structures (toroidal and plasmoidal) which were observed during the same shot (with a time delay of 30 ns), and constituted two steps of the internal structures evolution. In this paragraph, we described the evolution of the considered internal structures, especially during the periods of the fast electrons and ions acceleration [17].

Many interferometric images, which were recorded during the plasma radial implosion, showed usually the formation of two toroidal structures, which had some radial lobules in front of the imploding current sheath, at different positions along the z-axis. Some examples of such interferometric frames, are presented in Fig. 3.

The toroidal plasma structures were produced by a concentration of an initially smoothly-distributed azimuthal current, which was flowing in the column surface layer, into toroidal-like shape due to a tearing instability. Its larger radial radius in form of the lobules was caused by a repulsive pressure of the internal toroidal current, which limited the radial implosion. The upper lobule (L1 in Fig. 3b, c) separated a region of the dense plasma column from the umbrella-shaped part of the imploding current sheath. The top of that lobule showed also some transfer of denser plasma from the pinch column to the external low-density region, what could be deduced from shapes of the interferometric fringes visible behind the lobule tops (L1

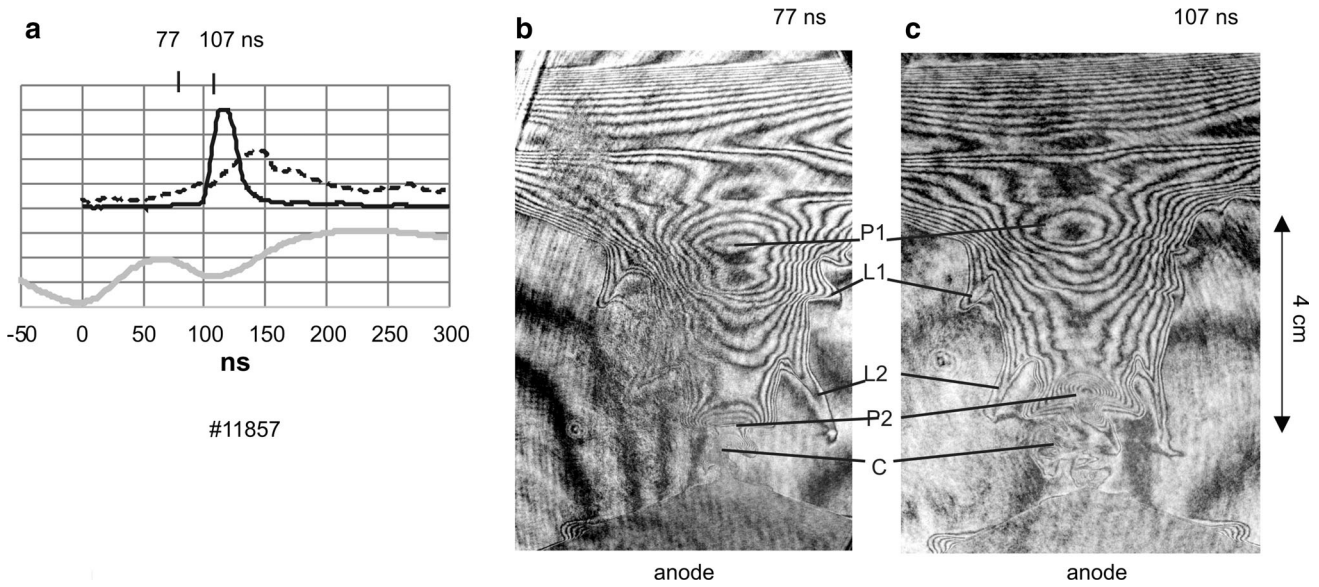


**Fig. 3** Shot #11857; **a** Waveforms of the current derivative (thick grey), HXRs (thin black) and fusion-neutrons (dashed) as a function of time. Interferometric images were recorded at instants marked above the waveforms. The interferometric frame **b** was taken before the HXR and neutron pulses, and an interruption of the pinch constriction, while the frame **c** was recorded at the explosion of the constriction and production of HXRs and neutrons. The symbols P1 and P2 indicate the plasmoids, L1 and L2 the lobules, and C the constriction

and L2). The first plasmoid (P1 in Fig. 3b, c) was generated in the z-position of the L1 lobule. It confined plasma escaping in the axial direction from the bottom region, in the period of the implosion stopping.

The formation of the first plasmoid P1 coincided usually with the production of the first HXR and neutron pulses. Their production could be caused by energy released during the spontaneous transformation of internal magnetic fields at reconnections of the magnetic lines.

The formation of the first plasmoid P1 in the pinch column coincided usually with the production of the first HXR and neutron pulses. Their production could be caused by energy released during the spontaneous transformation of internal magnetic fields at the reconnection of magnetic lines. It should be noted that the formation of the first plasmoid must not necessarily be accompanied by the HXR and neutron emission. For example, it does not occur at the presence of a conical tip upon the anode end-plate. During such discharges the plasmoid is usually characterized by smaller density gradients, and internal energy is confined inside the pinch column of a higher density for a longer time, until an instability is developed (see Fig. 3) [31]. It should also be mentioned that the HXR and neutron pulses were not recorded when the dense plasma structures were absent.

After the formation of the first plasmoid, the stagnation phase was started, in which the internal part of the dense plasma column with sparse interferometric fringes (between the plasmoid and the anode) transported its mass to the plasmoid. This phase was characterized both, by the radial expansion and by absence of internal gradients of a plasma density. They manifested the presence of an axial component of the magnetic field inside the dense column, which was associated with the azimuthal current flowing in the column boundary layer. The stagnation phase was ended after a few tens of ns by the stratification, when the initially smooth surface of the pinch column was subject to an evolution of the Reyleigh-Taylor instability, mainly due to the tearing instability accompanied by an axial fragmentation of the azimuthal current. Circumstances of the cascading of plasma structures to smaller dimensions were enabled by the mentioned submillimeter value of Larmor radius and mean free path of electron ion collisions.

After the described phase a part of the column imploded towards the z-axis, and formed the constrictions C (marked in Fig. 3b, c). This evolution was accompanied by an axial transport of plasma from the constriction C, firstly into the toroid which was converted gradually in the second plasmoid (P2 in Fig. 3b, c) formed above the z-position of the bottom lobule (L2). This transfer increased the internal mass and probably its poloidal current component, similarly as in the first plasmoid. One could suspect that the poloidal current was flowing from the anode near the plasmoidal boundary, as the main discharge current. In the near-axial region it was flowing in the opposite direction, toward the anode. This orientation could be a consequence of the penetration of the main discharge current (flowing in the column boundary) into the internal layers.

Possible schemes of transformations of the kinetic energy of plasma (incoming across and along the magnetic field lines) into the magnetic energy, when that plasma is confined inside the organized structures, is presented in Fig. 4a. At this time, the motion of plasma along the magnetic lines could transform the axial line into toroidal one, as shown in Fig. 4b.

At the confinement of incoming plasma inside plasmoids, its kinetic energy could be transformed into a chaotic turbulence, and subsequently into the magnetic energy of the ordered internal currents.

In Fig. 4a, the kinetic energy was transformed into magnetic one at the moving of the plasma perpendicularly to the primary magnetic field lines. Both fluids in frozen state drive into a rotation both around the velocity direction and around the initial direction of the B-field line. This motion created a ball of the magnetic lines, which conserved the magnetic energy. That spontaneous relaxing ball was a building element of the plasma organization process.

This transformation can be described (for a high Reynolds magnetic number) by the equation of plasma frozen in the magnetic field [13]:

$$\partial \boldsymbol{B}/\partial t = \mathrm{rot}(v \times \boldsymbol{B}) \tag{2}$$

The motion of plasma along the magnetic line, as shown in Fig. 4b, describe the transformation of the toroidal structure into plasmoidal one.

During the final phase of the pinched constriction there was observed the second stratification of the constriction surface along its length, when the secondary plasmoids were formed and some secondary constrictions appeared between them. A similar cascade process of the instability evolution to the smaller plasma structures was also observed and discussed in X-pinch experiments, or in solar flares [18, 19].

A relatively stationary first plasmoid living about few hundred ns, the generation of which was accompanied by the emission of the first neutron pulse, could be characterized by some balanced internal poloidal- and toroidal-components of the local magnetic field. The secondary plasmoid, as formed during the constriction compression, could be developed at a higher velocity. Its central poloidal current component could overcome the stationary value. Its pinching was subject to the evolution of instabilities and finally led to a release of the magnetic energy in a form of the induced electric field $\boldsymbol{E}$ (in opposite direction to the central current). This field accelerated beams of charged particles during reconnections of magnetic field-lines in the organized plasma structures, according the Faraday law and energy density balance:

$$-\partial \boldsymbol{B}/\partial t = \mathrm{rot}\,\boldsymbol{E} \quad \text{and} \quad B^2/2\mu \approx (1/2)\rho v^2 \tag{3}$$

where $\rho$ means the plasma mass density.

The plasma compression or expansion as well as the structures transformation inside the dense plasma column, which were observed in interferometric frames, occurred at the Alfvén velocity equal to (1–2) $\times$ $10^5$ m/s. The mean energy density, as determined from Eq. (3), corresponded to deuteron energy reaching a few hundreds of eV. This energy was evidently insufficient for the production of fusion neutrons. Higher energies of the charged particles, ranging hundreds keV, might be reached at the considerably higher energy density at the non-uniform structure of the current.

It is well known that the current flow in PF discharges has often a filamentary form [2, 20–24]. It can be observed on VUV frames, particularly in discharges performed with an admixture of the a gas with a higher Z. Some examples are imaged in Fig. 5.

The observed filamentation was supported by high values of the Prandtl number (i.e. the ratio of the magnetic and viscose characteristics, ranging up to 10), what was important for the generation of tangled currents in submillimeter scales [4]. Detailed characteristics of various plasma-current filaments, which were recorded in the PF-1000 experiments, were described in earlier papers [23, 24]. The tiny filaments presented in Fig. 5 connected the external layers of the dense column with internal

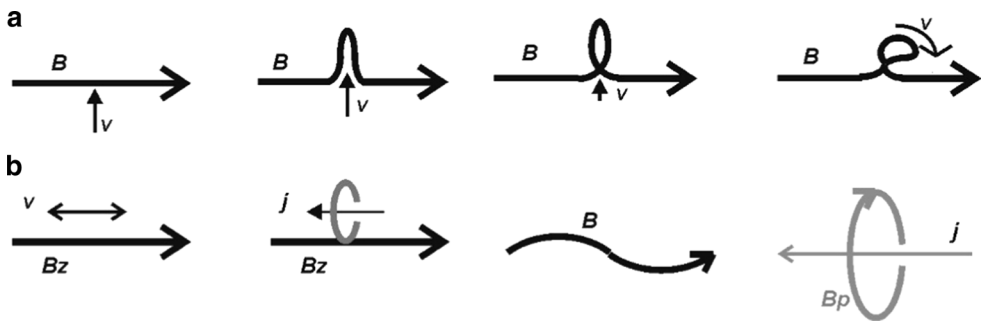


**Fig. 4** **a** Sketch of transformations of the kinetic energy into the magnetic one in the case of: transversal motion, and **b** sketch of the transformation of the axial magnetic line in toroidal at the longitudinal motion of plasma in relation to the magnetic line. Symbols: $\boldsymbol{v}$ the velocity of the plasma flow, $\boldsymbol{B}$ the magnetic field line, and $\boldsymbol{j}$ a current density

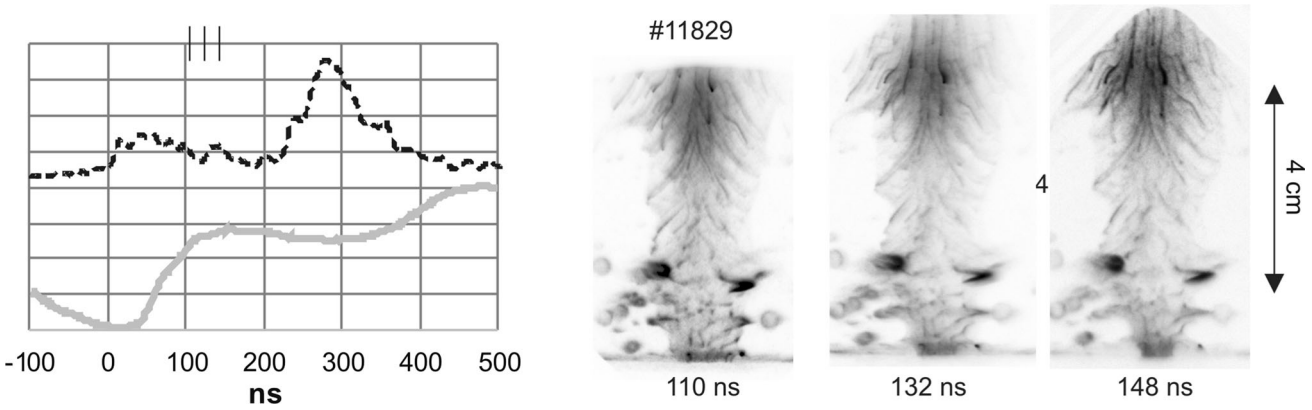


**Fig. 5** Shot #11829: (left) Waveforms of the current derivative (thick grey) and fusion-neutrons (dashed) as a function of time, and (right) numerous plasma filaments visible on the VUV frames recorded at different instants during the neutron production

structures and they presented the transport of energy from the external current to the plasmoid, namely during the period of neutron production. The acceleration of deuterons during a decay of the plasmoids might be explained, as mentioned above, by the coalescence of the current filaments inside these plasmoids, which have high densities of the kinetic and magnetic energies, as can be estimated from Eq. (3). For the deuteron velocity of order of $4 \times 10^6$ m/s, their kinetic energies can reach about 200 keV. At the electron density equal to $3 \times 10^{24}$ m$^{-3}$ and the magnetic field $B \approx 500$ T, such deuteron energies would be sufficient for production of the recorded fusion neutrons. Such a magnetic field might be produced, e.g., by current filaments of the radius equal to about 40 μm, which carry the current of about 70 kA [25]. The electric field intensity $\boldsymbol{E}$, as can be estimated from a linearized Faraday law, can reach the value $E \approx v \times B \approx 2 \times 10^9$ V/m.

The deuterons are accelerated in the developing and decaying plasmoids, and the generation of fusion neutrons is occurring in dense plasma contained inside the same or other plasmoids. A delay of the neutron production after the deuteron acceleration can be calculated by taking into account the mean velocity of fast deuterons (equal to about $4 \times 10^6$ m/s) and the distance between neighbour plasmoids, which is from 0 to 3 cm. This delay can amount to 10 ns, and corresponds to a delay of the neutron peak appearing after the HXR peak.

It should be noted that the recorded interferometric images did not provide any experimental information about the acceleration of charged particles in the interrupted pinch region of low-density plasma. However, a possibility of such acceleration of deuterons to MeV energies has been discussed for z-pinch discharges, e.g. in a paper [32].

## Examples of Organized Structures in Fusion Plasmas and Their Relations with Acceleration of Charged Particles

The questions of a fast release of the magnetic energy in the organized plasma structures, which might explain the non-thermal acceleration of energetic electron- and ion-beams, was also discussed in papers concerning other fusion and cosmic plasmas. For example, a dense plasma jet, which was produced by an intense laser beam focused upon a foil, was investigated by means of the laser interferometry and by the Faraday rotation method [26]. That jet was accompanied by a partially-closed poloidal current ranging hundreds kA and an azimuthal magnetic field of about 5 kT, which was observed in a sub-millimeter regions at the plasma density equal to about $10^{25}$ m$^{-3}$. Other laser experiment showed an attraction of two plasma jets (produced by two laser beams), whose coalescence and radiation could be interpreted by magnetic reconnections occurring in the sub-nanosecond scale [27]. The intense X-ray and neutron sources, which were observed in the NIF D-T fusion experiments [28], had the toroidal-like form oriented perpendicularly to the axis of the laser-irradiated pellet. In tokamak experiments the kinetic energy of charged particles, delivered by additional plasma heating systems, can be interpreted by conversion partially in the magnetic energy, which violates the smooth toroidal magnetic-flux surfaces. This energy is then periodically released in a form of the fast run-away electrons, which acceleration is interpreted also by magnetic reconnections. It enables to recover smooth surfaces of the magnetic fluxes repeatedly [29].

Therefore, the studies of organized plasma structures, their spontaneous evolution, and a release of the stored magnetic energy in the kinetic energy of fast charged particles, are important issues to be solved in the contemporary research on all fusion concepts. Also in cosmic

space, e.g. the solar flares are generated in regions of interactions of different magnetic tubes. The evolution of such structures is powered by magnetic reconnections which transform the initial magnetic energy into heat and kinetic energy during the formation of so-called flux ropes, cascades of plasmoids and flaring loops. These transformations have been studied by computer simulations of magnetic reconnections in 1D and 2D approaches, and during the recent years—also in a 3D model [19, 30]. Unfortunately, such models have not yet been developed for PF discharges.

The observations and hypotheses mentioned above are similar to the results of the described PF-1000 experiments. Therefore, the studies of different plasma organized structures and their transformations are of importance not only for laboratory plasma research, but also for the astrophysics.

## Summary and Conclusions

The most important results of this study can be summarized as follows: the convenient parameters of dense magnetized plasmas formed in PF-1000 device and the comprehensive diagnostics of a plasma density and a velocity of plasma column transformations, as well as the observed quasi-stationary states and short pulses of fast electrons and ions, made it possible to analyze the transformations of this fusion plasma, particularly during the periods of the emission of the fast electron- and ion-beams. The performed experiments proved the appearance of the toroidal and plasmoidal plasma structures, which were formed by closed internal currents with poloidal and toroidal components and their magnetic fields. Their spontaneous transformations have been explained by the magnetic dynamo and magnetic reconnections. Many experimental observations confirmed a filamentary structure of the current. The generation of fast particles was explained by the magnetic reconnections of the current filaments, in which a part of the magnetic energy was transformed into the accelerating electric field. It was noticed that the studies of laboratory fusion and cosmic plasmas solve similar problems, e.g. the fast release of the magnetic energy in a form of high-energy charged particles streams. A deeper collaboration of physicists engaged in the mentioned studies should give a new inspiration for reaching a desirable progress in the research on fusion plasma in a laboratory as well as astrophysical objects in space.

**Acknowledgements** This study was supported in part by the Research Program under Grants MSMT LTT17015, LTAUSA17084, CZ.02.1.01/0.0/0.0/16_019/0000778, GACR 16-07036S, IAEA CRP RC-19253, and SGS 16/223/OHK3/3T/13, as well by the Polish Ministry of Science and Higher Education within a framework of the financial resources allocated in 2018 for the realization of the international co-financed projects.

## References

1. M.G. Haines, Plasma Phys. Control. Fusion **53**, 093001 (2011)
2. A. Bernard, H. Bruzzone, P. Choi, H. Chaqui, V. Gribkov, J. Herrera, K. Hirano, A. Krejci, S. Lee, C. Luo, F. Mezzetti, M. Sadowski, H. Schmidt, K. Ware, C.S. Wong, V. Zoita, J. Moscow Phys. Soc. **8**, 93 (1998)
3. D.D. Ryutov, M.S. Derzon, M.K. Matzen, Rev. Mod. Phys. **72**, 167 (2000)
4. D.D. Ryutov, IEEE Trans. Plasma Sci. **43**, 2363 (2015)
5. M. Scholz, L. Karpinski, M. Paduch et al., Nukleonika **46**, 35 (2001)
6. M.J. Sadowski, M. Scholz, Nukleonika **47**, 31 (2002)
7. P. Kubes, M. Paduch, D. Klir, J. Kravarik, K. Rezac, I. Ivanova-Stanik, L. Karpinski, M.J. Sadowski, K. Tomaszewski, E. Zielinska, IEEE Trans. Plasma Sci. **39**, 672 (2011)
8. K. Rezac, D. Klir, P. Kubes, J. Kravarik, Plasma Phys. Controlled Fusion **54**, 105011 (2012)
9. E. Zielinska, M. Paduch, M. Scholz, Contrib. Plasma Phys. **51**, 279 (2011)
10. V.I. Krauz, K.N. Mitrofanov, M. Scholz, M. Paduch, L. Karpinski, E. Zielinska, P. Kubes, Plasma Phys. Control. Fusion **54**, 025010 (2012)
11. V.I. Krauz, K.N. Mitrofanov, M. Scholz, M. Paduch, L. Karpinski, E. Zielinska, P. Kubes, Europhys. Lett. **98**, 45001 (2012)
12. P. Kubes, M. Paduch, J. Cikhardt, B. Cikhardtova, D. Klir, J. Kravarik, K. Rezac, E. Zielinska, M.J. Sadowski, A. Szymaszek, K. Tomaszewski, D. Zaloga, Phys. Plasmas **24**, 072706 (2017)
13. T.G. Cowling, *Magnetohydrodynamics* (Adam Hilger Ltd., Bristol, 1976)
14. V.D. Shafranov, *Theory of Plasma Physics* (Gosatomizdat, Moscow, 1963) in Russian
15. P. Kubes, M. Paduch, B. Cikhardtova, J. Cikhardt, D. Klir, J. Kravarik, K. Rezac, J. Kortanek, E. Zielinska, M.J. Sadowski, A. Szymaszek, K. Tomaszewski, Phys. Plasmas **25**, 032706 (2018)
16. P. Kubes, V.I. Krauz, K. Mitrofanov, M. Paduch, M. Scholz, T. Pisarczyk, T. Chodukowski, Z. Kalinowska, L. Karpinski, D. Klir, J. Kortanek, E. Zielinska, J. Kravarik, K. Rezac, Plasma Phys. Control. Fusion **54**, 105023 (2012)
17. P. Kubes, D. Klir, J. Kravarik, K. Rezac, J. Kortanek, V. Krauz, K. Mitrofanov, M. Paduch, M. Scholz, T. Pisarczyk, T. Chodukowski, Z. Kalinowska, L. Karpinski, E. Zielinska, Plasma Phys. Control. Fusion **55**, 035011 (2013)
18. S.A. Pikuz, T.A. Shelkovenko, D.A. Hammer, Plasma Phys. Rep. **41**, 291 (2015)
19. M. Janvier, J. Plasma Phys. **83**, 535830101 (2017)
20. M. Sadowski, H. Herold, H. Schmidt, M. Shakhatre, Phys. Lett. **105A**, 117 (1984)
21. H. Schmidt, M. Sadowski, L. Jakubowski, E. Skladnik-Sadowska, J. Stanislawski, Plasma Phys. Control. Fusion **36**, 13 (1994)
22. M.J. Sadowski, M. Scholz, Nukleonika **57**, 11 (2012)
23. P. Kubes, D.M. Paduch, J. Cikhardt, B. Cikhardtova, E. Zielinska, Phys. Plasmas **21**, 122706 (2014)
24. P. Kubes, M. Paduch, J. Cikhardt, B. Cikhardtova, D. Klir, J. Kravarik, K. Rezac, E. Zielinska, M.J. Sadowski, A. Szymaszek, K. Tomaszewski, D. Zaloga, Phys. Plasmas **24**, 032706 (2017)
25. P. Kubes, M. Paduch, B. Cikhardtova, J. Cikhardt, D. Klir, J. Kravarik, K. Rezac, J. Kortanek, E. Zielinska, M.J. Sadowski, K. Tomaszewski, Phys. Plasmas **23**, 082704 (2016)

26. T. Pisarczyk, SYu. Guskov, T. Chodukowski et al., Phys. Plasmas **24**, 102711 (2017)
27. P.M. Nilson, L. Willingale, M.C. Kaluza et al., Phys. Rev. Lett. **97**, 255001 (2006)
28. H.-S. Park, O.A. Hurricane, D.A. Callahan et al., Phys. Rev. Lett. **112**, 055001 (2014)
29. M. Yamada, R. Kulsrud, H. Ji, Rev. Mod. Phys. **82**, 603 (2010)
30. Y. Su, A.M. Veronig, G.D. Holman et al., Nat. Phys. **9**, 2675 (2013)
31. P. Kubes, M. Paduch, J. Cikhardt, B. Cikhardtova, D. Klir, J. Kravarik, K. Rezac, E. Zielinska, M.J. Sadowski, A. Szymaszek, K. Tomaszewski, D. Zaloga, Phys. Plasmas **24**, 092707 (2017)
32. D. Klir, J. Cikhardt, B. Cikhardtova, J. Kravarik, P. Kubes, V. Munzar, K. Rezac, O. Sila, T. Hyhlik, J. Stodulka et al., New J. Phys. **20**, 053064 (2018)